Adsorption Forms of CO_2 on MIL-53(Al) and NH_2-MIL-53(Al) As Revealed by FTIR Spectroscopy

Mihaylov, Mihail; Chakarova, Kristina; Andonova, Stanislava; Drenchev, Nikola; Ivanova, Elena; Sabetghadam Esfahani, A.; Seoane de la Cuesta, B.; Gascon, J.; Kapteijn, Freek; Hadjiivanov, Konstantin

DOI
10.1021/acs.jpcc.6b07492

Publication date
2016

Document Version
Final published version

Published in
The Journal of Physical Chemistry C

THE JOURNAL OF PHYSICAL CHEMISTRY C

Article

pubs.acs.org/JPCC

Adsorption Forms of CO_2 on MIL-53(Al) and NH_2-MIL-53(Al) As Revealed by FTIR Spectroscopy

Mihail Mihaylov,[†] Kristina Chakarova,[†] Stanislava Andonova,[†] Nikola Drenchev,[†] Elena Ivanova,[†] Anahid Sabetghadam,[‡] Beatriz Seoane,[‡] Jorge Gascon,[‡] Freek Kapteijn,[‡] and Konstantin Hadjiivanov*[,†]

[†]Institute of General and Inorganic Chemistry, Bulgarian Academy of Sciences, Sofia 1113, Bulgaria

[‡]Catalysis Engineering, Chemical Engineering Department, Delft University of Technology, Julianalaan 136, 2628 BL Delft, The Netherlands

Supporting Information

ABSTRACT: Adsorption of CO_2 on MIL-53(Al) and NH_2-MIL-53(Al) has been studied by Fourier transform infrared (FTIR) spectroscopy at different temperatures and equilibrium pressures. For better interpretation of the spectra $^{13}CO_2$ was also utilized. It is established that with both samples at low coverages CO_2 forms O-bonded complexes with the structural OH groups (OH···$O^{12}CO$). These species are characterized by $\nu_3(^{12}CO_2)$ at 2337−2338 cm^{-1} and two $\nu_2(^{12}CO_2)$ modes around 662 and 650 cm^{-1}. Simultaneously, the ν(OH) modes of the hydroxyl groups are red-shifted, while the δ(OH) modes are blue-shifted. At higher coverages $(OH\cdots O^{12}CO)_2$ dimeric species are formed and this leads to a decrease of the $\nu_3(CO_2)$ frequency by 2−4 cm^{-1}. This change is due to vibrational interaction as proven by the observation that the frequency remains practically unaffected for (OH···$O^{12}CO$) (OH···$O^{13}CO$) dimeric species. Interaction between dimers leads to additional slight decrease of the value of $\nu_3(CO_2)$. In parallel with the CO_2 adsorption a partial transformation of the material from large-pore to narrow-pore form occurs. Far before CO_2 interacts with all hydroxyl groups, polymeric CO_2 species are produced within the MIL-53(Al) sample. They are characterized by a split $\nu_3(CO_2)$ mode with a pronounced component at 2340 cm^{-1}. The formation of these species involves some of the dimers and is accompanied by a reopening of the MIL-53 structure. Analysis of the shift of the OH modes led to the conclusion that the polymeric moiety interacts strongly with one OH group and more weakly with several other hydroxyls. No polymeric species were observed with the NH_2-MIL-53(Al) sample which is associated with the more stable narrow-pore structure of this material. However, evidence of interaction between CO_2 and the hydroxyls H-bonded to amino groups was found.

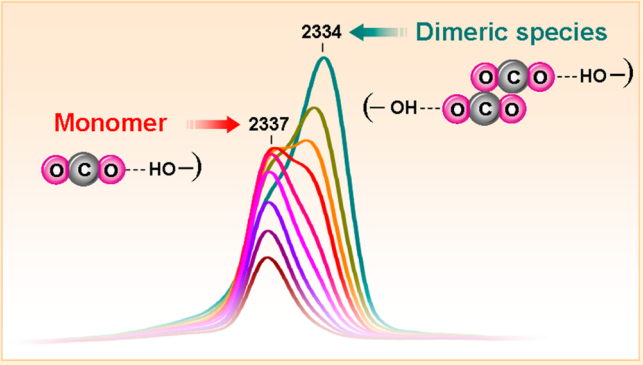

1. INTRODUCTION

Presently, one of the most widely used methods for CO_2 capture is its absorption in liquids. However, the process suffers from some drawbacks, e.g. contamination of the gas flow with solvent vapor and fast degradation of the absorbent. Porous materials, such as amine-functionalized silica, have been alternatively proposed. Recently, many hopes are concentrated on the development of metal−organic frameworks (MOFs) as (components of) materials for CO_2 capture.[1]

To be efficient, the adsorbent should bind CO_2 strongly enough, but on the other hand, the strength of adsorption should not be very high in order to allow easy regeneration. Therefore, detailed knowledge of the way of CO_2 interaction with different MOFs is of crucial importance. The problem is usually tackled by using complementary experimental in situ techniques (e.g., X-ray and neutron diffraction, Fourier transform infrared (FTIR), Raman, and solid state NMR spectroscopies, adsorption measurements) with theoretical modeling. Among the numerous investigations, valuable information can be obtained from vibrational spectroscopy studies. Irrespective of the serious achievements, however, many questions are still disputable and need resolving.

Carbon dioxide is a linear triatomic molecule with a $D_{\infty h}$ symmetry (d_{C-O} = 0.1163 nm). Although CO_2 has a zero dipole moment, it is a charge-separated molecule with significant nonzero bond dipole moments and a large quadrupole moment.[2] The CO_2 molecule possesses four fundamental modes:[2,3] ν_1 (symmetric stretchings); ν_2 (doubly degenerated bending vibrations), and ν_3 (antisymmetric stretching vibration). The ν_2 and ν_3 modes are infrared active, while ν_1 is only Raman active. For the free molecule in gas phase these modes appear at 1388.3 (ν_1), 667.3 (ν_2), and 2349.3 (ν_3) cm^{-1}.[3] In solid CO_2 ν_1 is detected by IR around 2344 cm^{-1}[4] while ν_2 splits into two components (659.8 and

Received: July 26, 2016
Revised: September 21, 2016
Published: September 29, 2016

DOI: 10.1021/acs.jpcc.6b07492
J. Phys. Chem. C 2016, 120, 23584−23595

Table 1. Spectral Data Reported after Interaction of CO_2 with OH Groups in MOFs

sample	OH group, cm^{-1}	$\Delta\nu$(OH), cm^{-1}	$\nu_3(CO_2)$, cm^{-1}	other CO_2 bands, cm^{-1}	note	ref
MIL-53(Cr)	3655	−19 to −22	2335	662, 653	up to 4 bar, NP form	25, 27, 28
		−13		659	5−10 bar, LP form	
MIL-53(Al)	3720	−38	2338	−	monomer	16
			2334.5		dimer	
MIL-53(Fe)-X, X = CH_3, Cl, Br	3650−3648	−28		661, 651	OH···O=C=O species + weak donor−acceptor interaction	29
NH_2-MIL-53(Al)	3700[a]	−28[a]	−	661, 649		31
MIL-125(Ti)	3686[a]	−54	ca. 2340		μ_2-OD···O=C=O	30
NH_2-MIL-125(Ti)	3686[a]	−41[a]	ca. 2340			30

[a]Experiments performed with deuterated samples. The values of ν(OH) and $\Delta\nu$(OH) are calculated from the respective ν(OD) and $\Delta\nu$(OD) values.

654.7 cm^{-1}) due to highly ordered structures (Davydov splitting).[5]

Because of the fact that the overtone of ν_2 almost coincides with the ν_1 mode, a Fermi resonance occurs and two bands of almost equal intensity are observed in the Raman spectrum at 1388 and 1285 cm^{-1}. The combination modes of these two bands with ν_3 give rise to two other bands at 3714 and 3612 cm^{-1}.[5]

Typical of CO_2 are also the so-called "hot" bands (excitation of already excited states) which are located at the low-frequency sides of the principal bands.[6] The relative intensity of these bands increases with temperature.

Upon coordination the molecule of CO_2 is affected thus producing changes in its spectral features. From a chemical point of view, CO_2 can act as an electron donor (through one or the two O atoms) and/or as electron acceptor (through the C atom). Upon coordination through the C atom the CO_2 molecule changes to a bent configuration. As a result, the ν_3 mode is significantly red-shifted, down to 1700 cm^{-1}.[5] At the same time, the ν_1 mode becomes IR active and is detected at 1400−1100 cm^{-1}. It is also considered that, because of the degeneration removal, two ν_2 bands are observed: in-plane (lower frequency) and out-of-plane (higher frequency) bending modes.[7−9] As will be discussed below, this statement needs some refinement.

When CO_2 is bonded through one of its oxygen atoms, the linearity of the molecule is preserved and the ν_1 mode remains IR silent. The reported data on the spectral performance of O-bonded species are controversial. There is strong evidence that formation of such complexes leads to a small red shift of the ν_3 mode (down to 2200 cm^{-1}).[5,10] However, matrix-isolation studies have indicated a moderate blue shift of ν_3 in M^+−OCO moieties (up to 2380 cm^{-1}).[11] Similar but less pronounced shift values have been reported when linear O-bonded species are formed with metal cations exchanged in zeolites.[12,13] These observations suggest that the increase of the C−O stretching frequency of the CO_2 molecule results from an electrostatic interaction (Stark effect). Indeed, the electrostatic interaction is expected to be strong in matrix-isolated cationic species as well as with CO_2 interacting with highly electrophilic cations in zeolites. When the electron transfer is essential, the ν_3 frequency should decrease.

An important question is the ν_3 reference value. It has been noted that the gas-phase frequency is not appropriate in this respect for the cases of porous materials because dispersion forces with the surrounding framework cause a red shift of the ν_3 mode. Consequently, a value of 2338 cm^{-1}, i.e. the ν_3 frequency of CO_2 adsorbed on silicalite and corrected for the interaction with silanols, is proposed as a reference.[14] A complication here is that the real reference value seems to depend on the pore dimensions. Thus, a significant effect was suggested for CO_2 in the small sodalite-like cages of $Ni_3(BTP)_2$, where weakly adsorbed CO_2 was detected at 2335 cm^{-1}.[15] In any case, considering a reference value differing from the gas phase frequency requires revision of many published data.

Usually CO_2 is weakly adsorbed on MOFs and the interaction is mainly electrostatic. Typical CO_2 adsorption sites are exposed metal cations and hydroxyl groups. Although with a lower interaction energy, CO_2 can be bound to other MOF sites, usually atoms from the organic linkers. When CO_2 interacts with the exposed metallic sites in MOFs, ν_3 frequencies in the range between 2353 (CPO-27-Mg) and 2334 cm^{-1} (Cu-BTC) have been reported.[7,14,17−25] When interacting with OH groups, ν_3 is observed in a narrow spectral interval, i.e. 2340−2335 cm^{-1} (see Table 1).[16,25,27−31]

Among different MOFs, these from the MIL-53 series (MIL stands for Matériaux de l'Institut Lavoisier) have been considered as promising materials for CO_2 storage and separation.[1,16,26−36] MIL-53 materials represent metal hydroxyterephthalates and are build up by infinite trans chains of corner-sharing $Me^{3+}O_4(OH)_2$ octahedra linked by 1,4-benzenedicarboxylate ligands.[31,35,38,39] They possess a three-dimensional skeleton structure with large pores up to 0.85 nm and are among the so-called breathing MOFs;[31,35] i.e. they switch between large-pore (LP) and narrow-pore (NP) forms upon adsorption or temperature changes. With the aim of developing more effective CO_2 adsorbents, NH_2-MIL-53(Al) MOF was synthesized.[35] This material exhibits the same topology as MIL-53(Al), but in this case the linker is the 2-aminoterephthalate anion.[31,35,38,39] Due to the H-bonding between the NH_2 and OH groups NH_2-MIL-53(Al) is in a very narrow-pore form.[31,39]

French authors studied in detail the adsorption of CO_2 on MIL-53(Cr).[26−28] They followed the process in a large pressure range at 305 K and compared the IR results with X-ray diffraction (XRD) data.[26,28] The activated material was in a LP form (diagnosed by the band at 1022 cm^{-1}), and CO_2 adsorption up to a pressure of 4 bar provoked transition to a NP form (band at 1017 cm^{-1}). At these conditions the ν_3 mode was observed at 2335 cm^{-1}[27] and two $\nu_2(CO_2)$ bands were detected at 662 and 650 cm^{-1}.[26,28] Simultaneously, a red shift by −22 cm^{-1} was observed for the ν(OH) band at 3655 cm^{-1} while the δ(OH) mode at 920 cm^{-1} appeared blue-shifted by 30 cm^{-1}. These spectral changes were associated with an

DOI: 10.1021/acs.jpcc.6b07492
J. Phys. Chem. C 2016, 120, 23584−23595

electron donor−acceptor interaction; the electron donor was identified as the oxygen atom from the OH group and the electron acceptor was the C atom from the CO_2 molecule. A complementary Raman study[32] registered the presence of the ν_1 and $2\nu_2$ bands at 1383 and 1281 cm^{-1}, respectively.

At higher CO_2 pressure (6−10 bar) the material was converted into the LP pore form (diagnostic band at 1022 cm^{-1}) and a new $\nu_2(CO_2)$ band appeared at 659 cm^{-1}.[26,28] Another set of shifts of the OH modes was associated with this band: $\Delta\nu(OH) = -13$ cm^{-1} and $\Delta\delta(OH) = 15$ cm^{-1}. Subsequent decrease in the pressure down to 2 mbar restored the spectrum initially recorded at low CO_2 pressure.

According to others,[33] at pressures lower than 6 bar one CO_2 molecule interacts with two OH groups on MIL-53(Cr), which explains the low ν_3 frequency of CO_2.

A series of studies on NH_2-MIL-53(Al) revealed two CO_2 adsorption forms.[31,34,35] The first form is associated with interaction of CO_2 with the OH groups that are not involved in H-bonding with NH_2 groups. In this case, two ν_2 bands were observed, at 661 and 649 cm^{-1}. In order to follow precisely the changes in the hydroxyl spectra, i.e. to prevent the hindering from the CO_2 combination modes, deuterated samples were investigated.[31] Upon CO_2 adsorption the OD band at 2726 cm^{-1} (corresponding to free hydroxyls observed at 3700 cm^{-1}) was shifted to 2705 cm^{-1}. The band at 2715 cm^{-1} (OD groups D-bonded to amino groups) was hardly affected. It was considered that these sites were occupied after breaking the preexisting D-bonds. In addition, only a negligible part of the NH_2 groups were affected by CO_2, presumably those located at the external surface.[35] Two $\nu_2(CO_2)$ bands were identified for this adsorption form, at 669 and 653 cm^{-1}.[38]

In the pilot communication of this study[16] we reported that low-temperature CO_2 adsorption on MIL-53(Al) leads, at low coverages, to formation of OH···OCO species characterized by a $\nu_3(CO_2)$ band at 2338 cm^{-1} and causing a shift of the 3720 cm^{-1} $\nu(OH)$ band by −38 cm^{-1}. At higher coverages $(OH\cdots OCO)_2$ dimers are produced which leads to a red shift of the $\nu_3(CO_2)$ by ca. −4 cm^{-1}. However, only one $\nu_3(^{13}CO_2)$ band (arising from the ^{13}C natural abundance) was registered at 2272 cm^{-1} for the two adsorption forms. This indicated that the shift of the $\nu_3(CO_2)$ was due to vibrational interaction. Moreover, we found that even at ambient temperature dimeric species could be formed.

In this work we explore our previous findings showing that the process is not restricted to MIL-53(Al) but can occur with different MOFs, in particular NH_2-MIL-53(Al). Moreover, here we demonstrate that at higher coverage polymers are formed with MIL-53(Al) and lead to opening of the structure. In contrast, no polymers are produced with NH_2-MIL-53 due to the relatively high stability of the narrow-pore form. We also provide detailed analysis of the whole spectral region, including the changes in the $\nu(OH)$ and $\delta(OH)$ regions as well as in the region of $\nu_2(CO_2)$ modes and offer more detailed information on the adsorbent−adsorbate and adsorbate−adsorbate interaction. For better assignment of the spectra, isotopically labeled CO_2 ($^{13}CO_2$) was used in the experiments.

2. EXPERIMENTAL SECTION

The MIL-53(Al) sample was a commercial BASF product Basolite A100. Before the experiments it was evacuated at 623 K for 30 min in order to remove the residual free acid. The amino-functionalized sample, NH_2-MIL-53(Al), was home-prepared, and synthesis details are reported elsewhere.[38] The sample was acid-free and was activated under vacuum at 473 K for 30 min.

The IR measurements were performed using Nicolet Avatar 360 and Nicolet 6700 FTIR spectrometers accumulating up to 128 scans at a spectral resolution of 2 cm^{-1} and accuracy of 0.01 cm^{-1}. Specially designed IR cells were used for the experiments. One of them, equipped with CaF_2 windows, allowed registering the spectra at low (100 K) and ambient temperatures. Another cell, equipped with KBr windows, allowed obtaining the spectra at a preset temperature in the range between 100 and 300 K. The cells were directly connected to a vacuum-adsorption apparatus with a residual pressure lower than 10^{-3} Pa.

To obtain the IR spectra the sample was spread onto a KBr pellet. This technique ensured optimal intensity of the IR bands. Parallel experiments were performed with a self-supporting pellet in order to verify the lack of interaction with KBr. During the low-temperature experiments helium was introduced in the cell before CO_2 adsorption in order to keep a constant temperature. Then CO_2 was introduced to the system and allowed to diffuse to the pellet. The background and gas-phase corrections were performed using Omnic software. For the low-temperature CO_2 experiments a spectrum registered in the presence of He was used as background.

Carbon dioxide (99.998% purity) was supplied by Messer. Labeled $^{13}CO_2$ (^{13}C isotopic purity of 99 atom %) was provided by Aldrich. Helium was supplied by Messer and had a purity of 99.999%.

3. EXPERIMENTAL RESULTS

3.1. Adsorption of CO_2 and $^{13}CO_2$ at Ambient Temperature. *3.1.1. Background Spectra.* The background spectra of the MIL-53(Al) and NH_2-MIL-53(Al) MOF compounds are already described in the literature,[16,31,34,35,37] and here we will only concentrate on the bands under interest for this study. Some details for the other regions are provided in the Supporting Information (see Figure S1).

The activated MIL-53(Al) sample shows two bands, at 1025 and 1019 cm^{-1}, which are indicative of the LP and NP forms of the material, respectively (Figure S1, spectrum a).[26] In the OH region, one band at 3708 cm^{-1} with a shoulder at 3702 cm^{-1} is recorded (see the inset in Figure S1). This band is attributed to $\nu(OH)$ of the structural μ_2-hydroxyl groups of the sample.[16,37] The heterogeneity is most probably associated with the coexistence of the LP and NP forms in the activated material. A component of the very intense (out of scale) band at ca. 986 cm^{-1} is due to the respective $\delta(OH)$ modes.

The spectrum of NH_2-MIL-53(Al), although similar, shows some differences. Due to the fact that the material is considered to be in a (very) NP form, there are no bands proposed to follow the pore structure. In the OH region two bands, at 3701 and 3681 cm^{-1}, are detected (Figure S1, spectrum c). The former band is due to (almost) free structural hydroxyl as found with the MIL-53(Al) sample. The band at 3681 cm^{-1} is attributed to structural hydroxyls involved in H-bonding with the amino groups.[31,34,35,37] The respective $\delta(OH)$ band was monitored by a component of the out-of-scale band around 987 cm^{-1}. In addition, two intense bands at 3500 and 3388 cm^{-1} are detected and assigned to the symmetric and antisymmetric N−H stretching modes of the amino groups.

3.1.2. Spectral Signatures of Adsorbed CO_2. First we compare the changes in the spectra occurring during adsorption of 50 mbar $^{12}CO_2$ or $^{13}CO_2$ at ambient temperature (298 K) on

DOI: 10.1021/acs.jpcc.6b07492
J. Phys. Chem. C 2016, 120, 23584−23595

the activated samples (Figure 1). Adsorption of $^{12}CO_2$ on MIL-53(Al) results in the appearance of a ν_3 band at 2336.1 cm^{-1}

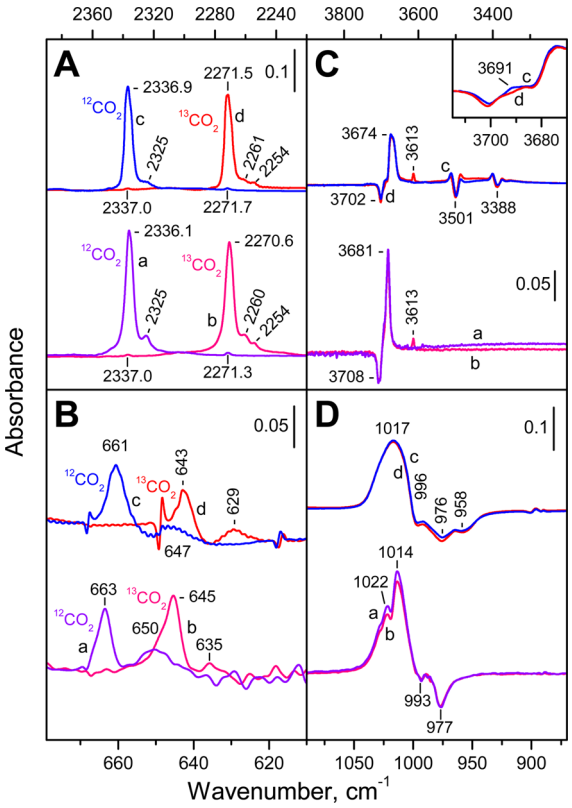

Figure 1. FTIR spectra recorded after ambient temperature adsorption of $^{12}CO_2$ (a, c) or ^{13}CO (b, d) (50 mbar equilibrium pressure) on MIL-53(Al) (a, b) and NH_2-MIL-53(Al) (c, d). The spectra are background and gas-phase corrected. Panel A, $\nu_3(CO_2)$ region; panel B, $\nu_2(CO_2)$ region; panel C, ν(OH)/ν(NH) region; and panel D, δ(OH) region.

(Figure 1A, spectrum a). Because the exact position of this band is essential for the following discussion, we will present the maximum values with the first figure after the decimal point which is allowed by the accuracy of our instrument. The ν_3 band has a pronounced shoulder at 2325 cm^{-1} which is assigned to the so-called "hot" band. A weak and broad band around 2370 cm^{-1} is most probably due to a combination mode. Another weak feature at 2271.3 cm^{-1} arises from the natural ^{13}C abundance and is attributed to the ^{13}C satellite of the principal band at 2336.1 cm^{-1}.

After adsorption of $^{13}CO_2$ the principal ν_3 band was detected at 2270.6 cm^{-1} (Figure 1A, spectrum b). The isotopic shift factor (i = 1.029) is in good agreement with the theoretical expectation (1.023). Note that the maximum of the main band is at slightly lower wavenumber as compared to the satellite $^{13}CO_2$ band recorded after adsorption of $^{12}CO_2$ at the same conditions. Comparison of the two bands after normalizing the intensity reveals a well-pronounced lower frequency component in the case of $^{13}CO_2$ adsorption (Figure S2, spectra a,b). The $^{13}CO_2$ "hot" band was detected at 2260 cm^{-1}, while the weak combination band appeared around 2304 cm^{-1}. Another band is well distinguished at ca. 2254 cm^{-1} and has no analogue in the spectrum of adsorbed $^{12}CO_2$. We attribute this band to small amounts of $^{13}C^{18}O^{16}O$ contaminants usually present in $^{13}CO_2$. Finally, a weak satellite $\nu_3(^{12}CO_2)$ band was detected at 2337.0 cm^{-1}. In this case again the band appears at a slightly higher wavenumber as compared to the same band detected after adsorption of pure $^{12}CO_2$ and the band contour indicates the absence of a lower-frequency shoulder.

Very similar results were obtained with the NH_2-MIL-53(Al) sample. The ν_3 band of adsorbed $^{12}CO_2$ (asymmetric from the low-frequency side) was registered at 2336.9 cm^{-1} and shifted to 2271.5 cm^{-1} upon $^{13}CO_2$ adsorption (Figure 1A, spectra c,d). Here again, the satellite bands were more symmetric and detected at slightly higher frequencies (2337.0 and 2271.7 cm^{-1}) but the effect was definitely less pronounced as compared to the MIL-53(Al) sample.

The spectra of the deformation CO_2 modes are noisier because of the presence of strong background bands in the region (Figure 1B). An intense band at 663 cm^{-1} and a weaker one at 650 cm^{-1} are recorded with the MIL-53(Al) sample. The two bands were shifted to 645 and 635 cm^{-1} when $^{13}CO_2$ was adsorbed. With the NH_2-MIL-53(Al) sample the bands were detected at slightly lower wavenumbers: 661 and 647 cm^{-1} ($^{12}CO_2$ adsorption) and 643 and 629 cm^{-1} ($^{13}CO_2$ adsorption). Note that additional heterogeneity of the adsorption forms is not excluded from the contour of the bands. A slight modulation around 668 cm^{-1} is observed in the spectra of adsorbed $^{12}CO_2$ (around 648 cm^{-1} for $^{13}CO_2$). This is attributed to the not efficient subtraction of the gas-phase likely due to a slight effect of the solid on a part of the gaseous CO_2 in vicinity. In all cases the isotopic shift factor for the ν_2 band (1.028−1.025) is consistent with the theoretical expectations. We have also found that the intensities of the lower-frequency bands do not decrease with temperature, which excludes their assignment to "hot" bands.

Analysis of the region of the combination modes of CO_2 is more difficult because of the superimposition with some OH and NH stretching bands. Relatively intense bands at 3613 cm^{-1} are detected in the spectra of $^{13}CO_2$ adsorbed on both samples (Figure 1C). These bands are absent from the spectra of adsorbed $^{12}CO_2$ and are attributed to the ν_1 + ν_3 combination modes. Taking into account the isotopic shift factor, the respective band for adsorbed $^{12}CO_2$ is expected around 3693 cm^{-1}. A careful inspection of the spectra indicated that indeed such features are observed but superimposed to the negative OH bands (see the inset in Figure 1C). The other combination band, $2\nu_2$ + ν_3, is of very low intensity and is distinguished in the spectra of adsorbed $^{12}CO_2$ around 3582 cm^{-1}.

In the 1400−1300 cm^{-1} region, where the ν_1 band is expected, some small deviations of the spectra, due to small changes in the intense background bands in this region, were detected (Figure S3). However, comparison between the spectra of the two adsorbed isotopologues ($^{12}CO_2$ and $^{13}CO_2$) indicated the lack of any bands assignable to the ν_1 and/or $2\nu_1$ modes. These results suggest that CO_2 is not bonded through its C atom.

Consider now the coverage effect. Here we will discuss mainly the ν_3 band because the deformation modes cannot be followed accurately due to their low intensities and the background changes. The spectra recorded with the MIL-53(Al) sample during the decrease of the CO_2 equilibrium pressure (initially adsorbed at 100 mbar) are shown in Figure 2A. It is seen that the ν_3 band decreases in intensity with the equilibrium pressure. At pressures of 10 mbar or lower the band maximum is practically coverage independent and is located at 2336.7 cm^{-1}. With the pressure increase the band maximum is

DOI: 10.1021/acs.jpcc.6b07492
J. Phys. Chem. C 2016, 120, 23584−23595

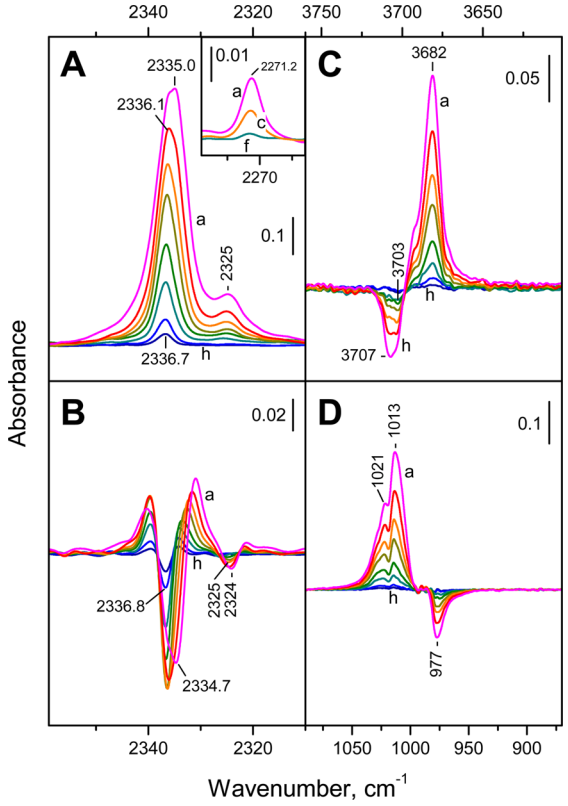

Figure 2. FTIR spectra recorded after adsorption of $^{12}CO_2$ on MIL-53(Al) at ambient temperature. Equilibrium $^{12}CO_2$ pressure of 100 (a), 50 (b), 30 (c), 20 (d), 10 (e), 5 (f), and 1 mbar (g) and after short evacuation (h). The spectra are background and gas-phase corrected. Panel A, $\nu_3(^{12}CO_2)$ region; panel B, second derivatives of the spectra presented in panel A; panel C, ν(OH) region; and panel D, δ(OH) region. The inset in panel A shows the $\nu_3(^{13}CO_2)$ region.

progressively shifted to lower frequencies, reaching the value of 2335.0 cm^{-1} at 100 mbar. In contrast, the maximum of the ^{13}C satellite ν_3 band remains almost unaffected by the equilibrium pressure (Figure 2A, inset).

In order to obtain more information on the phenomenon, we analyzed the second derivatives of the spectra (Figure 2B). It is clearly seen that a component at 2334.7 cm^{-1} develops with coverage increase while no similar changes were observed with the satellite ^{13}C band. Instead, a negligible red shift was detected. Differences between the spectra registered at decreasing coverages also support the above conclusions (Figure S4): development of a band around 2234.5 cm^{-1} at high coverages and erosion of the band at 2336.7 cm^{-1} (arrowed). These findings clearly show that the observed discrete red shift of the $\nu_3(^{12}CO_2)$ band with coverage increase is due to some kind of vibrational interaction.

The results obtained with $^{13}CO_2$ adsorption on MIL-53(Al) are in excellent agreement with the above conclusions. More details are provided in the Supporting Information (Figure S5).

The same phenomena were observed with the NH_2-MIL-53(Al) sample (Figure S6). Although in this case the effect of coverage on the band position was less pronounced, comparison of the normalized spectra clearly shows an additional low-frequency component under equilibrium pressure of 50 mbar as compared with the spectrum recorded under 10 mbar equilibrium pressure (Figure S6).

3.1.3. CO_2-Induced Changes in the Background Spectra. Adsorption of CO_2 or $^{13}CO_2$ on the MIL-53(Al) sample causes a red shift of the 3708 cm^{-1} band to 3681 cm^{-1} (Figures 1 and 2 and Figure S5). In this case it is preferable to analyze the changes caused by $^{13}CO_2$ adsorption in order to avoid the superimposition with the $\nu_1 + \nu_3$ combination band of $^{12}CO_2$. A careful analysis indicates that at lower coverages the shoulder at 3702 cm^{-1} is preferentially affected, followed by the band at 3708 cm^{-1}, but only one shifted band appears. The shifted band is more intense than the negative bands, which indicates formation of an H-bond. The CO_2 induced shift of the OH modes is between −21 and −28 cm^{-1}. This value is intermediate between the shifts caused by low-temperature adsorption of N_2 and CO (ca. −12 and −45 cm^{-1}, respectively)[37] and is consistent with the proton affinities of the three molecules.

Concerning the NH_2-MIL-53(Al) sample, the ν(OH) modes are also affected and the shifted band consists of two components: a main one at 3674 cm^{-1} and a shoulder at 3668 cm^{-1}. A careful analysis indicates that CO_2 affects mainly the original ν(OH) band at 3702 cm^{-1} and to a minor extent the band at 3681 cm^{-1}. However, it is not possible to relate the two shifted components to the two original OH bands. A more detailed interpretation will be offered below.

With the MIL-53(Al) sample a band at 977 cm^{-1} (OH deformation modes) is shifted to higher frequencies, but the shift (around +40 cm^{-1}) cannot be exactly determined because of the superimposition (Figure 2D). In any case, such a shift is expected to occur when an H-bond is formed. With the NH_2-MIL-53(Al) sample the shifted δ(OH) band is well detected at 1017 cm^{-1} (Figure 1D). A careful inspection of the spectra indicates some fine structure of the negative band which could suggest some heterogeneity of the affected hydroxyls. However, similar conclusions should be taken with care because false negative bands can be obtained when the principal band is out of scale.

The spectra presented in Figure 2 also indicate that a correlation exists between the intensities of the $\nu_3(CO_2)$ band and the shifted ν(OH) and δ(OH) bands. All these results, coupled with the absence of any IR active ν_1 mode, imply formation of OH···OCO complexes.

It is seen that the NH modes are also affected by CO_2 adsorption. However, compared to the OH groups, only a small fraction of the NH groups are involved in the process (see the intensities of the original bands, Figure S1). Analysis of the spectra indicates that the bands are rather broadened than shifted. Therefore, we have no evidence of direct bonding of CO_2 to the amino groups at these experimental conditions.

Finally, we tried to analyze the region around 1020 cm^{-1} modes indicative of NP and LP forms of the MIL-53(Al) material. However, because of the superimposition with the intense shifted δ(OH) bands, we were not able to draw definite conclusions from this set of experiments. However, analysis of another sensitive pair of bands (NP at 766 cm^{-1} and LP at 755 cm^{-1})[40] suggests that at high CO_2 equilibrium pressure a partial transformation of the material to the NP form occurs. These results are consistent with similar findings with a MIL-53-Cr sample.[26]

3.2. Low-Temperature Adsorption of CO_2. *3.2.1. Background Spectra.* Some background bands of many MOF materials are very sensitive to the temperature. In the low-temperature experiments, the actual temperature of the pellet depends on the pressure and the nature of the gas because

DOI: 10.1021/acs.jpcc.6b07492
J. Phys. Chem. C 2016, 120, 23584−23595

these parameters determine the thermal conductivity of the media. Therefore, during the low-temperature adsorption experiments, both temperature and adsorbate-induced effects are registered. In order to distinguish between them, the temperature effect should be well-known.

As seen from Figure S1, at low temperature (and in the presence of He) the bands due to isolated hydroxyls are shifted to higher frequencies and become narrower while the δ(OH) bands slightly shift to lower frequencies. This indicates that at room temperature these OH groups have been involved in weak H-bonds and the strength of this bond decreases at low temperature. Small deviations are observed with the MIL-53(Al) sample in the region of the δ(CH) modes of the terephthalate ligand around 1020 cm^{-1}. At low temperature the relative intensity of the band at 1024 cm^{-1} increases at the expense of the band at 1019 cm^{-1}, indicating increase of the fraction of the LP form.

3.2.2. Spectral Signatures of Adsorbed CO_2. Immediately after introduction of CO_2 at 100 K to the MIL-53(Al) sample, a broad band at 2338.8 cm^{-1} develops (Figure 3, spectra a,b).

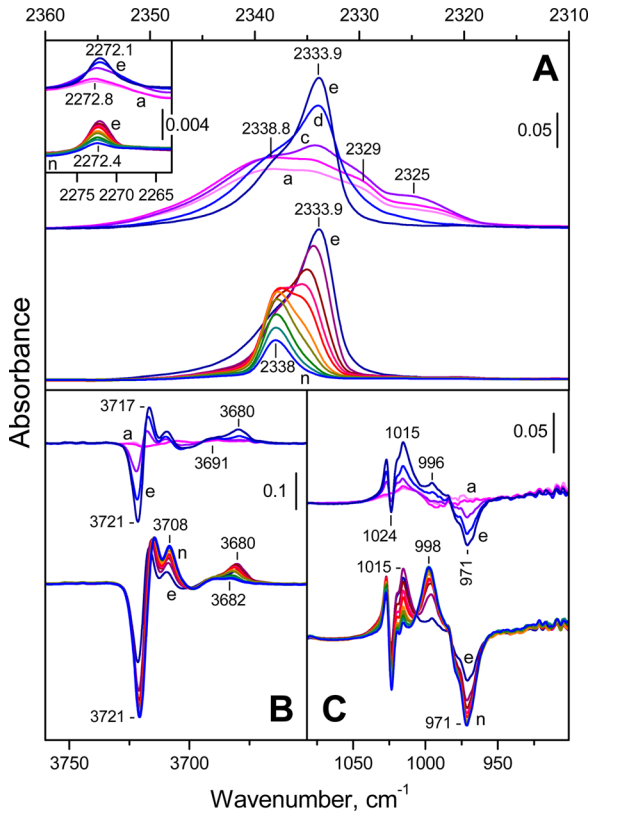

Figure 3. FTIR spectra recorded after low-temperature adsorption of $^{12}CO_2$ on MIL-53(Al). Initial equilibrium $^{12}CO_2$ pressure of 5 mbar (a), after 5 min (b), and evolution of the spectra during evacuation at 100 K (c–n). The spectra are background and gas-phase corrected. Panel A, $\nu_3(^{12}CO_2)$ region; panel B, ν(OH) region; panel C, δ(OH) region. The inset in panel A shows the $\nu_3(^{13}CO_2)$ region.

The band has lower frequency shoulders located at 2334, 2329, and 2325 cm^{-1}. The background spectra are only slightly affected. We assign the broad band to the ν_3 modes of weakly adsorbed CO_2. The relatively high wavenumber of this band indicates the lack of pore effects. This, coupled with the fact that the OH groups remain practically unaffected, indicates the band is due to CO_2 adsorbed on the external MOF surface. These conclusions are supported by analysis of the region of deformation modes: two bands at 661 and 655 cm^{-1}, typical of solid CO_2, were observed (not shown). Subsequent evacuation at 100 K leads to fast disappearance of the broad feature around 2339 cm^{-1} and development of a sharp $\nu_3(^{12}CO_2)$ band at 2333.9 cm^{-1} (Figure 3, spectra c–e). Additional evacuation (Figure 3, spectra f–n) causes decrease in intensity of the band at 2333.9 cm^{-1} and development, at its expense, of another band at 2338.0 cm^{-1}. The latter one further decreases in intensity without changing its position. These spectral changes are typical of conversion between monomeric and dimeric surface species.[41,42]

Consider now the changes of the satellite $^{13}CO_2$ band. Normally, it is expected that this band should demonstrate the same behavior as the respective $^{12}CO_2$ band if no vibrational interaction occurs. However, at the initial stages of adsorption the position of the satellite band was at 2272.8 cm^{-1} (broad band due to weakly adsorbed molecules on the external surface) and then shifted to 2272.1 cm^{-1}. Further evacuation led to a decrease in intensity of the band and a negligible shift of its maximum to 2272.4 cm^{-1}. These results demonstrate that the two bands, around 2338 cm^{-1} (higher frequency, or HF) and 2334 cm^{-1} (lower frequency, or LF), are characterized by only one $^{13}CO_2$ satellite band around 2272.4–2272.1 cm^{-1}.

Very similar results were obtained with the NH_2-MIL-53 sample (Figure 4). At the initial stages of adsorption a broad

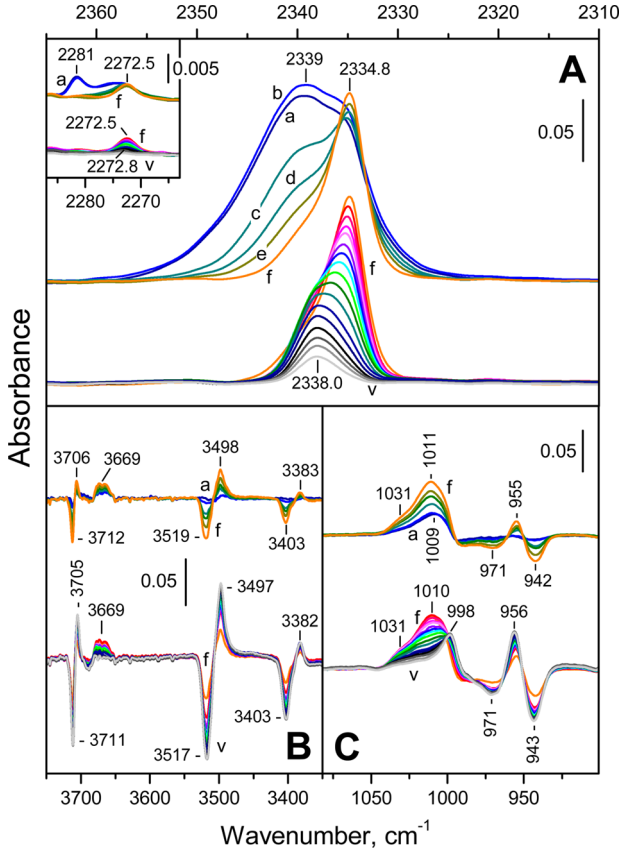

Figure 4. FTIR spectra recorded after adsorption of $^{12}CO_2$ on NH_2-MIL-53(Al). Initial equilibrium $^{12}CO_2$ pressure of 5 mbar (a), after 5 min (b), and evolution of the spectra during evacuation at 100 K (c–v). The spectra are background and gas-phase corrected. Panel A, $\nu_3(^{12}CO_2)$ region; panel B, ν(OH)/ν(NH) region; panel C, δ(OH) region. The inset in panel A shows the $\nu_3(^{13}CO_2)$ region.

DOI: 10.1021/acs.jpcc.6b07492
J. Phys. Chem. C 2016, 120, 23584–23595

band at 2339 cm^{-1} with shoulders at 2336 and 2335 cm^{-1} developed. Here again, the background spectrum was hardly affected. Evacuation leads first to development of a LF band at 2334.8 cm^{-1} which then decreases in intensity and is converted to another, HF band at 2338.0 cm^{-1}. Note that in this case the difference between the HF and LF bands is slightly smaller. In the ^{13}C satellite region initially a band at 2281 cm^{-1} with a lower frequency shoulder at 2274 cm^{-1} appeared immediately after CO_2 adsorption. During evacuation a band at 2272.5 cm^{-1} developed and then declined, slightly shifting to 2272.8 cm^{-1}. Here again, the HF and LF bands (2234.8 and 2238 cm^{-1}) had only one $^{13}CO_2$ satellite band.

It is clearly seen that for the two samples conversion between two adsorption forms occurs and the phenomenon is due to interaction between adsorbed CO_2 molecules. The maximal integral intensities of the HF bands are roughly 2 times lower than those of the LF bands, which suggests that the species formed at high coverage can be associated with structures involving two CO_2 molecules. The appearance of only one ν_3 band for these dimeric species shows that the CO_2 molecules are equivalent; i.e., the complex formed is symmetric.

In dimeric structures practically all $^{13}CO_2$ molecules due to ^{13}C natural abundance should have $^{12}CO_2$ neighbors. The fact that after the removal of solid-like CO_2 the $\nu_3(^{13}CO_2)$ frequency remains coverage independent indicates that the $\nu_3(^{12}CO_2)$ frequency change is due to some kind of vibrational interaction. This interaction is more pronounced with the MIL-53(Al) sample.

3.2.3. CO_2-Induced Changes in the Background Spectra. The initial stages of low-temperature CO_2 adsorption of MIL-53(Al) hardly affect the hydroxyl bands (Figure 3B, spectra a,b). During the subsequent evacuation, the band at 3721 cm^{-1} is progressively eroded until the end of the experiments (corresponding to a very low CO_2 coverage). Simultaneously, several bands at lower frequencies develop: at 3717−3714, 3708, 3691, and 3682−3679 cm^{-1}. However, these bands show different behaviors. The former two bands (3717−3714 and 3708 cm^{-1}) continuously rise in the course of the experiments. In more detail, the band is slightly red-shifted (development of the component at 3717−3714 cm^{-1}) and part of it is converted into a band at 3708 cm^{-1}. Similar effects were observed during evacuation of He put in contact with MIL-53(Al) at 100 K and are thus attributed to temperature changes. In contrast, the other two bands (at 3691 and 3682−3679 cm^{-1}) start to develop with the LF $\nu_3(CO_2)$ band at ca. 2334 cm^{-1}. The band at 3691 cm^{-1} is of very weak intensity and very rapidly reaches a saturation level. The behavior of the band around 3680 cm^{-1} is more complicated. Initially observed at 3679 cm^{-1}, it reaches a maximum practically together with the band at 2334 cm^{-1}. Then it starts to decrease, shifting to 3682 cm^{-1}. The process seems to coincide with the conversion of the LF band at 2334 cm^{-1} to the HF band at 2338 cm^{-1}. Therefore, we can conclude that the number of affected OH groups practically coincides with the number of chemisorbed CO_2 molecules (2338−2334 cm^{-1}) irrespective of the adsorption form (monomers or dimers). Another important conclusion is that at these experiments only part of the hydroxyls were affected by CO_2 adsorption probably due to blocking of part of the pores.

The changes in the δ(OH) region are consistent with these observations (Figure 3C). First, a negative band around 971 cm^{-1} continuously develops and can be related to the negative ν(OH) band at 3721 cm^{-1}. Another band at 996−998 cm^{-1} develops in parallel and is associated with the 3708 cm^{-1} stretching band (temperature change). Finally, a band around 1015 cm^{-1} can be assigned to deformation modes of hydroxyls H-bonded to CO_2.

Consider now the NH_2-MIL-53(Al) sample. In this case again the background was weakly affected during the initial stages of CO_2 adsorption (Figure 4). With evacuation two types of changes occur. The changes associated with the temperature rise are progressive shifts of the following: (i) the ν(OH) band at 3712 cm^{-1} to 3706−3705 cm^{-1}; (ii) the δ(OH) band at 943 cm^{-1} to 956 and 998 cm^{-1}, and (iii) the ν(NH) bands at 3517 and 3403 cm^{-1} to 3497 and 3382 cm^{-1}, respectively. A synchrony between the intensities of the shifted bands at 998 and 3703 cm^{-1} is seen. In addition, a broad band at 3669 cm^{-1} with a high-frequency shoulder is formed. Here again the band reaches maximal intensity in concert with the CO_2 band at ca. 2334 cm^{-1} and the OH deformation band at 1011 cm^{-1} and these bands are associated with H-bonded CO_2.

3.3. Adsorption of CO_2 at Intermediate Temperature. *3.3.1. Sample MIL-53(Al).* In order to verify that the LF−HF band conversion and the behavior of the $\nu_3(^{13}CO_2)$ band are due to vibrational interaction, we comparatively studied the adsorption of $^{13}CO_2$ alone as well as that of a 1:1 $^{12}CO_2$ + $^{13}CO_2$ isotopic mixture. These experiments were performed at higher temperature, ca. 200 K, in order to avoid the formation of solid-like CO_2. Another aim of these studies is to reach higher CO_2 coverages that were not possible to attain at ambient temperature (due to thermodynamic reasons) and at low temperature (attributed to blocking of the pores).

Consider first the spectra at relatively low coverages. If a 1:1 $^{12}CO_2$ + $^{13}CO_2$ mixture is adsorbed, statistically the isotopic composition of the dimers formed should be 25% $(^{12}CO_2)_2$, 50% $(^{12}CO_2)(^{13}CO_2)$, and 25% $(^{13}CO_2)_2$. Therefore, if our conclusions were true, the LF band should be related only to $(^{13}CO_2)_2$ species and thus should appear with strongly reduced relative intensity in the spectra of the isotopic mixture. In contrast, monomeric and $(^{12}CO_2)(^{13}CO_2)$ dimeric species should be responsible for the development of the HF band.

The spectra presented in Figure 5A,B fully support this statement. Indeed, it is seen that the LF band is much more pronounced when pure $^{13}CO_2$ was adsorbed. Surprisingly, the LF band was additionally red-shifted with coverage increase (Figure 5A, spectrum f). In order to follow more precisely these changes, we analyzed the second derivatives of the spectra (Figure 5C,D). Consider first the HF band. It is practically coverage independent in the spectra of adsorbed $^{13}CO_2$. A slight red shift is observed in the spectra of adsorbed isotopic mixture which is associated with the contribution of mixed dimers to this band and indicates that the vibrational interaction between $^{12}CO_2$ and $^{13}CO_2$, although negligible, is not absent. Note that this is the reason for the already noted very slight red shift of the satellite bands.

The LF band only slightly shifts with coverage increase when the isotopic mixture is adsorbed. However, the shift is more essential in the spectra of adsorbed $^{13}CO_2$ (1.6 cm^{-1}). Analysis of the ν(OH), δ(OH), and $\nu_2(CO_2)$ regions did not show any additional peculiarities. These results imply that with coverage increase additional vibrational interaction occurs and indicate formation of some kind of oligomeric species.

We discuss now the changes occurring at higher coverage. In these cases the $\nu_3(^{13}CO_2)$ band was of very high intensity and out of scale (Figure 6A). Second derivatives (see Figure 6A,inset) indicate development of a high frequency component located at 2275.0 cm^{-1} (2340.3 cm^{-1} for adsorbed $^{12}CO_2$).

DOI: 10.1021/acs.jpcc.6b07492
J. Phys. Chem. C 2016, 120, 23584−23595

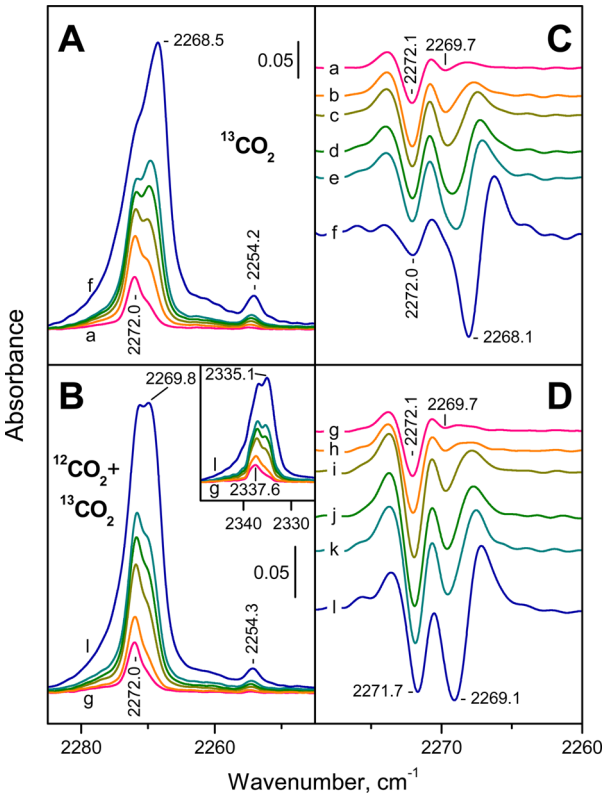

Figure 5. FTIR spectra in the $\nu_3(^{13}CO_2)$ region recorded after adsorption of $^{13}CO_2$ (panel A) and $^{12}CO_2$ + $^{13}CO_2$ (1:1 molar ratio) isotopic mixture (panel B) on MIL-53(Al) at 200 K. The spectra (a–f) and (g–l) are obtained after successive adsorption of small doses of CO_2 and correspond to similar total coverages (controlled by the intensity of the bands in the OH region). All spectra are background and gas-phase corrected. Panels C and D represent the second derivatives of the spectra shown in panels A and B, respectively. The inset in panel B depicts the $\nu_3(^{12}CO_2)$ region.

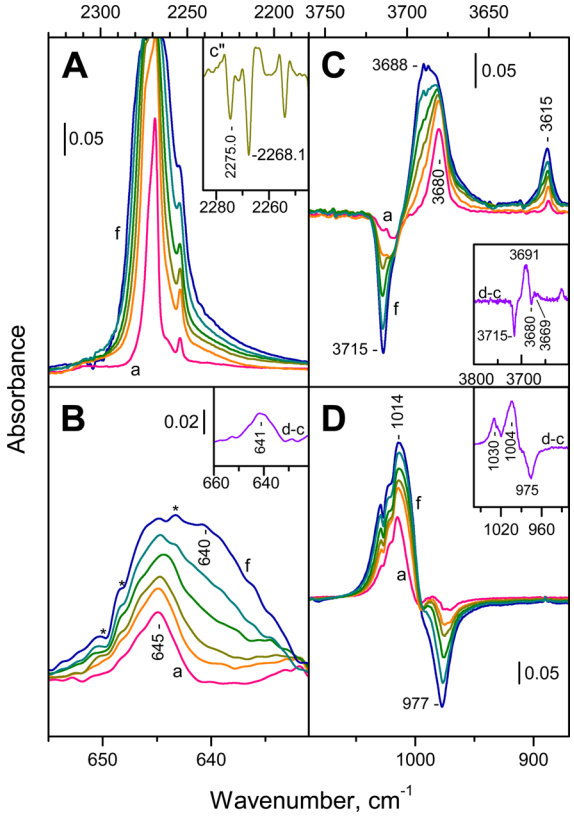

Figure 6. FTIR spectra recorded after adsorption of $^{13}CO_2$ on MIL-53(Al) at 200 K (continuation from Figure 5). The spectra (a–f) are obtained after successive adsorption of small doses of $^{13}CO_2$ and are background and gas-phase corrected. Panel A, $\nu_3(^{13}CO_2)$ region; panel B, $\nu_2(^{13}CO_2)$ region; panel C, ν(OH) region; and panel D, δ(OH) region. The inset in panel A shows the second derivative of spectrum c. The insets in panels B, C, and D show the difference "d–c" spectrum in the respective regions. All spectra are background and gas-phase corrected. The asterisks in panel B show peaks due to nonefficient $^{13}CO_2$ gas-phase subtraction.

Although, due to superimposition, the band attributed to $^{13}C^{18}O^{16}O$ at ca. 2254 cm^{-1} cannot be precisely followed, it is clearly seen that it is hardly affected by coverage. A high-frequency component of the ν_1 + ν_3 combination band also develops at 3614.2 cm^{-1}.

In the low-frequency region a new $\nu_2(^{13}CO_2)$ band appeared at 640 cm^{-1}. Although superimposed to the ν_2 bands produced at lower coverage, the band is well seen in the difference spectrum (Figure 6B, inset). When $^{12}CO_2$ was adsorbed, the band was registered at 658 cm^{-1}.

Consider now the hydroxyl bands. At the highest coverage practically all OH groups are affected by adsorbed CO_2. However, in this case the CO_2-induced shift of ν(OH) is smaller. The difference spectrum (inset in Figure 6C) clearly shows the consumption of a component at 3715 cm^{-1} and development of a broader band at 3691 cm^{-1} ($\Delta\nu$(OH) = −23 cm^{-1}). A negative band at 3680 cm^{-1} is also seen, confirming the decrease in concentration of the dimeric species at high coverage. In agreement with these changes, the shift of the δ(OH) modes is also reduced; $\Delta\delta$(OH) = −30 cm^{-1} (see the inset in Figure 6D).

Similar results, although with different shift values, were earlier reported with MIL-53(Cr) sample (in this case the hydroxyls are of lower acidity as compared to the hydroxyls in MIL-53(Al)).[26] A careful analysis of our spectra reveals additional small bands (at ca. 3674 and 1030 cm^{-1}) representing decreasing shifts of both ν(OH) and δ(OH) modes (−40 and −65 cm^{-1}, respectively). All these findings indicate that at high coverage new polymeric species are formed. It seems that these species interact strongly with one (or a few) OH group while the interaction with the other hydroxyls is weakened. Although the polymers are produced at the expense of the dimers and/or oligomers, the latter species have not fully disappeared even after all OH groups were affected by CO_2. Finally, we note that the relative intensity of the $^{13}CO_2$ combination band at 3615 cm^{-1} is relatively high, which suggests that not all of the $^{13}CO_2$ molecules from the polymeric species are bonded to OH groups.

3.3.2. Sample NH_2-MIL-53(Al). The conversion between monomeric and dimeric CO_2 species on NH_2-MIL-53(Al) was confirmed in a set of experiments, as already observed with MIL-53(Al) (see Figure S7).

Figure 7 shows the spectral changes occurring after CO_2 adsorption at 200 K on NH_2-MIL-53(Al) at increasing coverages up to the coverage when almost all "free" OH groups are affected. It is clear that no polymers are formed in this case. This is seen by the absence of both a new $\nu_2(CO_2)$ band (Figure 7B) and a low-frequency component of the shifted ν(OH) band (Figure 7B). A careful analysis of the spectra shows that, at high coverage, the 3684 cm^{-1} hydroxyls

DOI: 10.1021/acs.jpcc.6b07492
J. Phys. Chem. C 2016, 120, 23584–23595

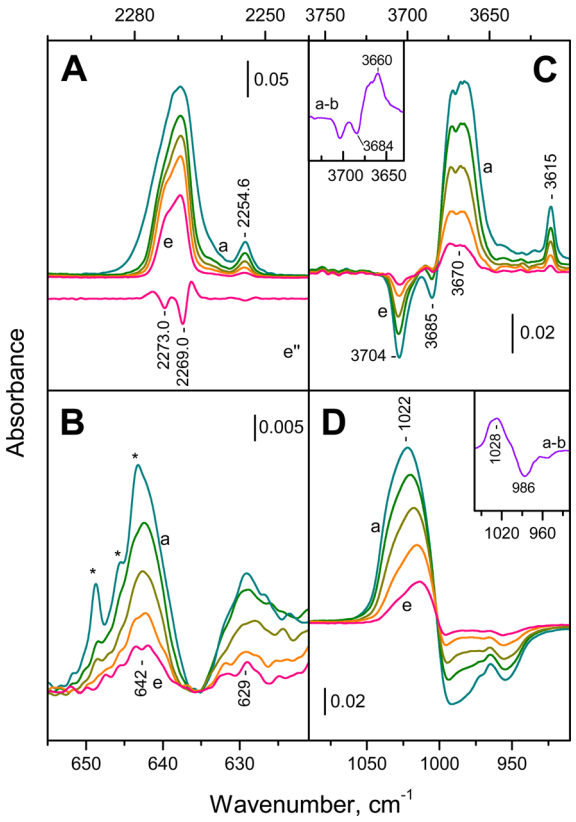

Figure 7. FTIR spectra recorded after adsorption of $^{13}CO_2$ on NH_2-MIL-53(Al) at 200 K. The spectra are obtained after introduction of $^{13}CO_2$ (2 mbar) at 200 K to the sample (a) followed by progressive evacuation at the same temperature (b–e). Panel A, $\nu_3(^{13}CO_2)$ region; panel B, $\nu_2(^{13}CO_2)$ region; panel C, ν(OH) region; and panel D, δ(OH) region. The insets in panels C and D show difference "a–b" spectra in the respective regions. All spectra are background and gas-phase corrected. The asterisks in panel B show peaks due to nonefficient $^{13}CO_2$ gas-phase subtraction.

are also affected by CO_2. Normally, one could expect that the formation of a new H-bond should lead to the breaking of the preexisting H-bond with the amino group. However, the results demonstrate that this is not the case. The difference spectra shown in the insets in Figure 7C,D show that the shifted ν(OH) band is at 3660 cm^{-1}, i.e. at position lower by 10 cm^{-1} than the band of the shifted "free" hydroxyls. This is attributed to the formation of bifurcated complexes;[37] i.e., the proton of the OH group is bonded to two additional atoms. The conclusion is confirmed by the spectra in the δ(OH) region where a component of the shifted band at 1028 cm^{-1} is clearly observed. However, in any case the preexisting H-bond is considerably weakened which is consistent with the low stability of the complexes formed.

4. DISCUSSION

4.1. Monomeric Species. The experiments described in this work, as well as analysis of the literature data, show that, at low CO_2 uptake, complexes between CO_2 and the structural OH groups of the investigated MOFs are formed. The spectral performance of these species is summarized in Table 2.

The shift of ν(OH) depends on the proton affinity (PA) of the guest molecule. The PA of CO_2 (540 kJ mol^{-1}) is intermediate between the PAs of N_2 (494 kJ mol^{-1}) and CO (594 kJ mol^{-1}), which means that the CO_2-induced shift should be intermediate between the N_2- and CO-induced shifts. Note that coordination of an electron acceptor to the O atom from a hydroxyl group should also lead to a red shift of the ν(OH) modes. However, this shift is much smaller as compared to the shift caused by the formation of H-bond.[43] Indeed, it is considered that formation of a very strong bond with a metal cation (passing from I to II and III type hydroxyls) leads to a decrease in the OH stretching frequency by ca. 50 cm^{-1}.[43] Therefore, weak interaction with guest molecules should result in a much smaller shift.

Not only with our samples, but also with other MOFs, CO_2 adsorption causes a red shift of the $\nu_3(CO_2)$ mode with respect to the gas-phase CO_2 frequency (see Table 1). However, the value is close to the reference value proposed for CO_2 sorbed in porous materials and we can stress that this mode is negligibly blue-shifted upon adsorption. This conclusion is consistent with the low adsorption enthalpy of CO_2.

Note also that no IR active ν_1 mode was observed with CO_2 on the two samples, which strongly indicates that the CO_2 molecule is not bonded through the C atom. However, two ν_2 bands were detected in each case. Usually, the split of ν_2 is considered as strong evidence of formation of C-bonded CO_2 due to the lowering of the symmetry and removal of the degeneracy of the deformation modes. We discuss now the possible reasons for this contradiction.

Table 2. Spectral Signatures of the Different CO_2 Adsorption Complexes Observed in This Study

sample	$\nu_3(^{12}CO_2)$, cm^{-1}	$\nu_2(^{12}CO_2)$, cm^{-1}	ν(OH), cm^{-1}	δ(OH), cm^{-1}
		Monomers, OH···OCO		
MIL-53(Al)	2337.0 (298 K)	663, 650	3680	ca. 1014
	2337.4 (200 K)			
	2338.0 (100 K)			
NH_2-MIL-53(Al)	2337.0 (298 K)	661, 643	3674–3668	1018–1011
	2338.0 (100 K)			
		Dimers, $(OH···OCO)_2$		
MIL-53(Al)	2334.7 (298 K)	663, 650	3683	ca. 1014
	2334.1 (200 K)			
	2333.9 (100 K)			
NH_2-MIL-53(Al)	2334.5 (298 K)	661, 643	3674–3668	1018–1011
	2334.8 (100 K)			
		Polymers, $OH(CO_2)_x(OH)_{x-1}$		
MIL-53(Al)	2340.3 + (?) (200 K)	658	3691 + 3668 (w)	1004 + 1030 (w)

DOI: 10.1021/acs.jpcc.6b07492
J. Phys. Chem. C 2016, 120, 23584–23595

A bent triatomic molecule (e.g., H_2O) has only three vibration modes.[3] Therefore, the appearance of two deformation modes for adsorbed CO_2 cannot be simply related to the symmetry lowering. Evidently, the symmetry of the entire adsorption complex should be taken into account.

Consider first the situation of C-bonded CO_2 (Scheme 1, left). Even if the linearity of the molecule is hardly affected, the deformation modes could be split into two components, in-plane and out-of-plane vibrations (visualized by differently colored arrows). However, a nonlinear O-bonded complex should also demonstrate similar in-plane and out-of-plane deformation modes (Scheme 1, right). Therefore, taking into account the above discussion, we conclude that at low coverage bent OH···OCO species (OH···O angle ≠ 180°) are formed. For both samples they are characterized by a ν_3 mode at 2337 cm^{-1} which is slightly shifted, to 2338 cm^{-1}, at low temperature.

Scheme 1. Split of the ν_2 Mode of Adsorbed CO_2 into In-Plane and Out-of-Plane Vibrations When Forming C-Bonded and Nonlinear O-Bonded Complexes[a]

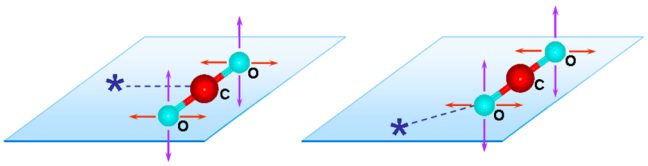

[a]The adsorption site is denoted by an asterisk. The plane is determined by the two oxygen atoms and the adsorption site. In both cases the CO_2 molecule is presented as linear.

4.2. Dimeric Species. The spectra presented in Figures 3 and 4 clearly demonstrate conversion between two types of CO_2 adsorption species attributed to monomers and dimers. It was also established that in the two cases each CO_2 molecule is connected to one OH group. On the basis of these results and parallel DFT studies, we have proposed the structure presented in Scheme 2. The interaction between the two CO_2 molecules is weak, which is seen by the negligible effect on the $\nu_3(^{13}CO_2)$ modes associated with the ^{13}C natural abundance. The appearance of a LF band for the dimeric species is due to vibrational interaction between two $^{12}CO_2$ molecules.

Scheme 2. Dimeric CO_2 Species Formed in the Pores of MIL-53(Al)

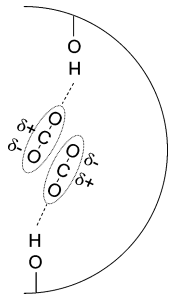

It also appears that the ν_3 frequency of the dimers is slightly temperature dependent (see Table 2). Moreover, the difference between the HF and LF bands also seems to decrease with temperature increase, which could be related to higher kinetic energy of the molecules.

4.3. Polymeric Species. The experiments performed at 200 K with the MIL-53(Al) sample indicated that, after dimeric species were formed, additional vibrational interaction leads to supplementary red shift of the $\nu_3(CO_2)$ bands attributed to formation of oligomers. These could be trimers. However, it is more probably that two dimers interact vibrationally because we have not observed clear conversion between dimeric and eventual trimeric species.

Consider now the polymers formed in MIL-53(Al) at high CO_2 coverage. They have several pronounced peculiarities. First, they are characterized by a $\nu_3(CO_2)$ band at higher wavenumbers (2340.3 cm^{-1} for $^{12}CO_2$). Unfortunately, due to the very high intensities and superimposition, we are not able to determine all bands characteristic of the polymeric species. However, difference spectra suggested the existence of low-frequency features which indicates a split of the $\nu_3(CO_2)$ band into two or more components.

The change of the values of the CO_2-induced shifts of the ν(OH) and δ(OH) modes at high CO_2 coverages is an interesting phenomenon. At first sight (and discarding the weak OH band at 3669 cm^{-1} demonstrating an enhanced shift) the phenomenon can easily be attributed to heterogeneity of the hydroxyl groups: initially the most acidic hydroxyls are affected followed by the less acidic ones. However, this explanation is not consistent with the experimental observation for several reasons: (i) only one type of structural hydroxyls is expected for MIL-53(Al), (ii) the hydroxyl band at ca. 3680 cm^{-1} is formed with the different hydroxyl bands in the 3720−3708 cm^{-1} region (expected to be involved in different H-bonds with the framework before CO_2 adsorption), and (iii) no similar heterogeneity has been seen using CO and N_2 as molecular probes. In addition, the partial destruction of the dimeric species indicates formation of a new type of bonding with the hydroxyls.

Our result can be rationalized by the assumption that the polymeric structures formed interact simultaneously with several OH groups. However, the interaction with one (or a few) hydroxyl is enhanced leading to a relatively large shift of the OH band. Consequently, the interaction with the rest of the OH groups is weakened.

Similar results were previously reported with a MIL-53(Cr) sample where a decreased shift of the OH modes and a new $\nu(CO_2)$ band were associated with a new adsorption form and reopening of the MOF structure. In our case we are not able to make definite conclusions on the pore structure, especially at high CO_2 coverages, because of the band superimposition. Indeed, due to the higher acidity of the hydroxyls in the aluminum-containing MIL-53 (compared to MIL-53-Cr), the shifted δ(OH) band masks the pore-diagnostic bands around 1020 cm^{-1}. However, the very similar frequencies of adsorbed CO_2 strongly support the idea that at high CO_2 pressure MIL-53(Al) is also converted in a LP form. These results are in full agreement with the absence of polymeric species in the NH_2-MIL-53(Al) sample, which is consistent with the relatively stable narrow-pore form of this material.

In conclusion, the present work clarifies a row of questions on the spectral performance of CO_2 adsorbed in porous materials. We also provide an easy IR tool for distinguishing between monomeric and dimeric CO_2 species in MOFs. Although here we report on two samples, MIL-53(Al) and NH_2-MIL-53(Al), we have observed similar phenomena with other MOF materials, which suggests that the reported dimerization and polymerization of adsorbed CO_2 are not

DOI: 10.1021/acs.jpcc.6b07492
J. Phys. Chem. C 2016, 120, 23584−23595

isolated phenomena. Finally, our results throw light upon the mechanism of adsorbate-induced phase transition of MOFs.

■ ASSOCIATED CONTENT

Supporting Information

The Supporting Information is available free of charge on the ACS Publications website at DOI: 10.1021/acs.jpcc.6b07492.

Background IR spectra and IR spectra of adsorbed $^{12}CO_2$ and $^{13}CO_2$ (PDF)

■ AUTHOR INFORMATION

Corresponding Author

*E-mail: kih@svr.igic.bas.bg. Tel.: +35 9 2 979 35 98.

Notes

The authors declare no competing financial interest.

■ ACKNOWLEDGMENTS

The research leading to these results has received funding from the European Union Seventh Framework Programme (FP7/2007-2013) under Grant Agreement No. 608490, project M4CO2. The authors thank Prof. M. Daturi for some helpful discussion.

■ REFERENCES

(1) Sumida, K.; Rogow, D. L.; Mason, J. A.; McDonald, T. M.; Bloch, E. D.; Herm, Z. R.; Bae, T.-H.; Long, J. R. Carbon Dioxide Capture in Metal-Organic Frameworks. *Chem. Rev.* **2012**, *112*, 724−781.

(2) Herzberg, G. *Molecular Spectra and Molecular Structure*; van Nostrand Reinhold: New York, 1950.

(3) Nakamoto, K. *Infrared Spectra of Inorganic and Coordination Compounds*, 2nd ed.; Wiley-Interscience: New York, 1970.

(4) Isokoski, K.; Poteet, C. A.; Linnartz, H. Highly Resolved Infrared Spectra of Pure CO_2 Ice (15−75 K). *Astron. Astrophys.* **2013**, *555*, A85.

(5) Aresta, M.; Angelini, A. The Carbon Dioxide Molecule and the Effects of Its Interaction with Electrophiles and Nucleophiles. *Top. Organomet. Chem.* **2015**, *53*, 1−38.

(6) Sathyanarayana, D. N. *Vibrational Spectroscopy: Theory and Applications*; New Age International Publishers: New Delhi, 2015.

(7) Yao, Y.; Nijem, N.; Li, J.; Chabal, Y. J.; Langreth, D. C.; Thonhauser, T. Analyzing the Frequency Shift of Physiadsorbed CO_2 in Metal Organic Framework Materials. *Phys. Rev. B: Condens. Matter Mater. Phys.* **2012**, *85*, 064302.

(8) Culp, J. T.; Goodman, A. L.; Chirdon, D.; Sankar, S. G.; Matranga, C. Mechanism for the Dynamic Adsorption of CO_2 and CH_4 in a Flexible Linear Chain Coordination Polymer as Determined from In Situ Infrared Spectroscopy. *J. Phys. Chem. C* **2010**, *114*, 2184−2191.

(9) Kauffman, K. L.; Culp, J. T.; Goodman, A.; Matranga, C. FT-IR Study of CO_2 Adsorption in a Dynamic Copper(II) Benzoate-Pyrazine Host with CO_2-CO_2 Interactions in the Adsorbed State. *J. Phys. Chem. C* **2011**, *115*, 1857−1866.

(10) Castro-Rodriguez, I.; Nakai, H.; Zakharov, L. N.; Rheingold, A. L.; Meyer, K. Linear, O-Coordinated η^1-CO_2 Bound to Uranium. *Science* **2004**, *305*, 1757−1759.

(11) Walker, N. R.; Walters, R. S.; Duncan, M. A. Infrared Photodissociation Spectroscopy of $V^+(CO_2)_n$ and $V^+(CO_2)_nAr$ complexes. *J. Chem. Phys.* **2004**, *120*, 10037−10045.

(12) Bonelli, B.; Civalleri, B.; Fubini, B.; Ugliengo, P.; Otero Areán, C.; Garrone, E. Experimental and Quantum Chemical Studies on the Adsorption of Carbon Dioxide on Alkali-Metal-Exchanged ZSM-5 Zeolites. *J. Phys. Chem. B* **2000**, *104*, 10978−10988.

(13) Montanari, T.; Busca, G. On the Mechanism of Adsorption and Separation of CO_2 on LTA Zeolites: An IR Investigation. *Vib. Spectrosc.* **2008**, *46*, 45−51.

(14) Valenzano, L.; Vitillo, J. G.; Chavan, S.; Civalleri, B.; Bonino, F.; Bordiga, S.; Lamberti, C. Structure−Activity Relationships of Simple Molecules Adsorbed on CPO-27-Ni Metal−Organic Framework: In Situ Experiments vs. Theory. *Catal. Today* **2012**, *182*, 67−79.

(15) Shearer, G. C.; Colombo, V.; Chavan, S.; Albanese, E.; Civalleri, B.; Maspero, A.; Bordiga, S. Stability vs. Reactivity: Understanding the Adsorption Properties of $Ni_3(BTP)_2$ by Experimental and Computational Methods. *Dalton Trans.* **2013**, *42*, 6450−6458.

(16) Mihaylov, M.; Chakarova, K.; Andonova, S.; Drenchev, N.; Ivanova, E.; Pidko, E. A.; Sabetghadam, A.; Seoane, B.; Gascon, J.; Kapteijn, F.; Hadjiivanov, K. Adsorption of CO_2 on MIL-53(Al): FTIR Evidence of the Formation of Dimeric CO_2 Species. *Chem. Commun.* **2016**, *52*, 1494−1497.

(17) Llewellyn, P. L.; Bourrelly, S.; Serre, C.; Vimont, A.; Daturi, M.; Hamon, L.; De Weireld, G.; Chang, J. S.; Hong, D.-Y.; Hwang, Y. K.; Jhung, S. H.; Férey, G. High Uptakes of CO_2 and CH_4 in Mesoporous Metals Organic Frameworks MIL-100 and MIL-101. *Langmuir* **2008**, *24*, 7245−7250.

(18) Leclerc, H.; Vimont, A.; Lavalley, J.-C.; Daturi, M.; Wiersum, A. D.; Llwellyn, P. L.; Horcajada, P.; Férey, G.; Serre, C. Infrared Study of the Influence of Reducible Iron(III) Metal Sites on the Adsorption of CO, CO_2, Propane, Propene and Propyne in the Mesoporous Metal−Organic Framework MIL-100. *Phys. Chem. Chem. Phys.* **2011**, *13*, 11748−11756.

(19) Miller, S. R.; Alvarez, E.; Fradcourt, L.; Devic, T.; Wuttke, S.; Wheatley, P. S.; Steunou, N.; Bonhomme, C.; Gervais, C.; Laurencin, D.; Morris, R. E.; Vimont, A.; Daturi, M.; Horcajada, P.; Serre, C. A Rare Example of a Porous Ca-MOF for the Controlled Release of Biologically Active NO. *Chem. Commun.* **2013**, *49*, 7773−7775.

(20) Bordiga, S.; Regli, L.; Bonino, F.; Groppo, E.; Lamberti, C.; Xiao, B.; Wheatley, P. S.; Morris, R. E.; Zecchina, A. Adsorption Properties of HKUST-1 toward Hydrogen and Other Small Molecules Monitored by IR. *Phys. Chem. Chem. Phys.* **2007**, *9*, 2676−2685.

(21) Dietzel, P. D. C.; Johnsen, R. E.; Fjellvag, H.; Bordiga, S.; Groppo, E.; Chavan, S.; Blom, R. Adsorption Properties and Structure of CO_2 Adsorbed on Open Coordination Sites of Metal−Organic Framework Ni_2(dhtp) from Gas Adsorption, IR Spectroscopy and X-Ray Diffraction. *Chem. Commun.* **2008**, *44*, 5125−5127.

(22) Miller, S. R.; Pearce, G. M.; Wright, P. A.; Bonino, F.; Chavan, S.; Bordiga, S.; Margiolaki, I.; Guillou, N.; Férey, G.; Bourrelly, S.; Llewellyn, P. L. Structural Transformations and Adsorption of Fuel-Related Gases of a Structurally Responsive Nickel Phosphonate Metal-Organic Framework, Ni-STA-12. *J. Am. Chem. Soc.* **2008**, *130*, 15967−15981.

(23) Valenzano, L.; Civalleri, B.; Chavan, S.; Palomino, G. T.; Areán, C. O.; Bordiga, S. Computational and Experimental Studies on the Adsorption of CO, N_2, and CO_2 on Mg-MOF-74. *J. Phys. Chem. C* **2010**, *114*, 11185−11191.

(24) Masala, A.; Vitillo, J. G.; Bonino, F.; Manzoli, M.; Grande, C. A.; Bordiga, S. New Insights into UTSA-16. *Phys. Chem. Chem. Phys.* **2016**, *18*, 220−227.

(25) Cabello, C. P.; Rumori, P.; Turnes Palomino, G. Carbon Dioxide Adsorption on MIL-100(M) (M = Cr, V, Sc) Metal−Organic Frameworks: IR Spectroscopic and Thermodynamic Studies. *Microporous Mesoporous Mater.* **2014**, *190*, 234−239.

(26) Serre, C.; Bourrelly, S.; Vimont, A.; Ramsahye, N. A.; Maurin, G.; Llewellyn, P. L.; Daturi, M.; Filinchuk, Y.; Leynaud, O.; Barnes, P.; Férey, G. An Explanation for the Very Large Breathing Effect of a Metal−Organic Framework during CO_2 Adsorption. *Adv. Mater.* **2007**, *19*, 2246−2251.

(27) Vimont, A.; Travert, A.; Bazin, P.; Lavalley, J.-C.; Daturi, M.; Serre, C.; Ferey, G.; Bourrelly, S.; Llewellyn, P. L. Evidence of CO_2 Molecule Acting as an Electron Acceptor on a Nanoporous Metal−Organic-Framework MIL-53 or $Cr^{3+}(OH)(O_2C-C_6H_4-CO_2)$. *Chem. Commun.* **2007**, *43*, 3291−3293.

(28) Bourrelly, S.; Serre, C.; Vimont, A.; Ramsahye, N. A.; Maurin, G.; Daturi, M.; Filinchuk, Y.; Férey, G.; Llewellyn, P. L. A Multidisciplinary Approach to Understanding Sorption Induced Breathing in the Metal Organic Framework MIL53(Cr). In *From*

DOI: 10.1021/acs.jpcc.6b07492
J. Phys. Chem. C 2016, 120, 23584−23595

Zeolites to Porous MOF Materials − the 40th Anniversary of International Zeolite Conference; Xu, R., Gao, Z., Chen, J., Yan, W., Eds.; Elsevier: Amsterdam, 2007; pp 1008−1014.
(29) Devic, T.; Salles, F.; Bourrelly, S.; Moulin, B.; Maurin, G.; Horcajada, P.; Serre, C.; Vimont, A.; Lavalley, J.-C.; Leclerc, H.; Clet, G.; Daturi, M.; Llewellyn, P. L.; Filinchuk, Y.; Férey, G. Effect of the Organic Functionalization of Flexible MOFs on the Adsorption of CO_2. *J. Mater. Chem.* **2012**, *22*, 10266−10273.
(30) Vaesen, S.; Guillerm, V.; Yang, Q.; Wiersum, A. D.; Marszalek, D.; Gil, B.; Vimont, A.; Daturi, M.; Devic, T.; Llewellyn, P. L.; Serre, C.; Maurin, G.; De Weireld, G. A Robust Amino-Functionalized Titanium(IV) Based MOF for Improved Separation of Acid Gases. *Chem. Commun.* **2013**, *49*, 10082−10084.
(31) Serra-Crespo, P.; Gobechiya, E.; Ramos-Fernandez, E. V.; Juan-Alcañiz, J.; Martinez-Joaristi, A.; Stavitski, E.; Kirschhock, C. E. A.; Martens, J. A.; Kapteijn, F.; Gascon, J. Interplay of Metal Node and Amine Functionality in NH_2-MIL-53: Modulating Breathing Behavior through Intra-framework Interactions. *Langmuir* **2012**, *28*, 12916−12922.
(32) Hamon, L.; Llewellyn, P. L.; Devic, T.; Ghoufi, A.; Clet, G.; Guillerm, V.; Pirngruber, G. D.; Maurin, G.; Serre, C.; Driver, G.; van Beek, W.; Jolimaître, E.; Vimont, A.; Daturi, M.; Férey, G. Co-Adsorption and Separation of CO_2-CH_4 Mixtures in the Highly Flexible MIL-53(Cr) MOF. *J. Am. Chem. Soc.* **2009**, *131*, 17490−17499.
(33) Vitillo, J. G.; Savonnet, M.; Ricchiardi, G.; Bordiga, S. Tailoring Metal−Organic Frameworks for CO_2 Capture: The Amino Effect. *ChemSusChem* **2011**, *4*, 1281−1290.
(34) Couck, S.; Denayer, J. F. M.; Baron, G. V.; Rémy, T.; Gascon, J.; Kapteijn, F. An Amine-Functionalized MIL-53 Metal-Organic Framework with Large Separation Power for CO_2 and CH_4. *J. Am. Chem. Soc.* **2009**, *131*, 6326−6327.
(35) Stavitski, E.; Pidko, E. A.; Couck, S.; Remy, T.; Hensen, E. J. M.; Weckhuysen, B. M.; Denayer, J.; Gascon, J.; Kapteijn, J. Complexity behind CO_2 Capture on NH_2-MIL-53(Al). *Langmuir* **2011**, *27*, 3970−3976.
(36) Deniz, E.; Karadas, F.; Patel, H. A.; Aparicio, S.; Yavuz, C. T.; Atilhan, M. A Combined Computational and Experimental Study of High Pressure and Supercritical CO_2 Adsorption on Basolite MOFs. *Microporous Mesoporous Mater.* **2013**, *175*, 34−42.
(37) Mihaylov, M.; Andonova, S.; Chakarova, K.; Vimont, A.; Ivanova, E.; Drenchev, N.; Hadjiivanov, K. An Advanced Approach for Measuring Acidity of Hydroxyls in Confined Space: a FTIR Study of Low-Temperature CO and $^{15}N_2$ Adsorption on MOF Samples from the MIL-53(Al) Series. *Phys. Chem. Chem. Phys.* **2015**, *17*, 24304−24314.
(38) Gascon, J.; Aktay, U.; Hernandez-Alonso, M. D.; Van Klink, G. P. M.; Kapteijn, F. Amino-Based Metal-Organic Frameworks as Stable, Highly Active Basic Catalysts. *J. Catal.* **2009**, *261*, 75−87.
(39) Seoane, B.; Téllez, C.; Coronas, J.; Staudt, C. NH_2-MIL-53(Al) and NH_2-MIL-101(Al) in Sulfur-Containing Copolyimide Mixed Matrix Membranes for Gas Separation. *Sep. Purif. Technol.* **2013**, *111*, 72−81.
(40) Salazar, J. M.; Weber, G.; Simon, J. M.; Bezverkhyy, I.; Bellat, J. P. Characterization of Adsorbed Water in MIL-53(Al) by FTIR Spectroscopy and Ab-Initio Calculations. *J. Chem. Phys.* **2015**, *142*, 124702.
(41) Hadjiivanov, K.; Knözinger, H. FTIR Spectroscopic Evidence of Formation of Geminal Dinitrogen Species during the Low-Temperature N_2 Adsorption on NaY Zeolites. *Catal. Lett.* **1999**, *58*, 21−26.
(42) Hadjiivanov, K.; Ivanova, E.; Klissurski, D. Site-Specified and Complex-Specified Formation of Geminal Species during Adsorption of Small Molecules on Cationic Sites. *Catal. Today* **2001**, *70*, 73−82.
(43) Hadjiivanov, K. Identification and Characterization of Surface Hydroxyl Groups by Infrared Spectroscopy. *Adv. Catal.* **2014**, *57*, 99−318.

DOI: 10.1021/acs.jpcc.6b07492
J. Phys. Chem. C 2016, 120, 23584−23595